Ordering of Air-Oxidized Decanethiols on Au(111)

Kai Sotthewes,*,[†,‡] Özlem Kap,[†,¶] Hairong Wu,[†,⊥] Damien Thompson,[§] Jurriaan Huskens,[‖] and Harold J. W. Zandvliet[†]

[†]Physics of Interfaces and Nanomaterials, and [‖]Molecular Nanofabrication, MESA+ Institute for Nanotechnology, University of Twente, P. O. Box 217, 7500AE Enschede, The Netherlands
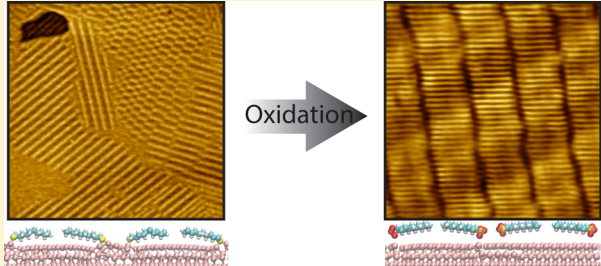
[‡]II. Institute of Physics B and JARA-FIT, RWTH—Aachen University, 52056 Aachen, Germany

[¶]Department of Materials Science and Engineering, Izmir Institute of Technology, Urla 35430, İzmir, Turkey

[§]Department of Physics, Bernal Institute, University of Limerick, Limerick V94 T9PX, Ireland

Ⓢ Supporting Information

ABSTRACT: Self-assembled monolayers (SAMs) of alkanethiols on gold are a commonly used platform for nanotechnology owing to their ease of preparation and high surface coverage. Unfortunately, the gold—sulfur bond is oxidized at ambient conditions which alters the stability and structure of the monolayer. We show using scanning tunneling microscopy and X-ray photoelectron spectroscopy that decanethiolate molecules oxidize into decanesulfonates that organize into a hitherto unknown striped phase. Air-exposed SAMs oxidize, as can be determined by a shift of the S 2p peak and the appearance of O 1s photoelectrons as part of the decanethiol monolayer transforms into a lamellae-like decanesulfonate structure when exposed to air. The herringbone structure of the Au(111) surface is preserved, indicating that the interaction between the molecules and the surface is rather weak as these findings are substantiated by density functional theory calculations.

INTRODUCTION

The self-assembly of organosulfur molecules on Au(111) surfaces has been a topic of intense research during the past few decades. Organosulfur self-assembled monolayers are easy to prepare and are useful for many technological applications ranging from molecular electronics to immobilization of biological molecules.[1−4] In order to incorporate self-assembled monolayers (SAMs) into functional electronic devices, a fundamental and detailed understanding of the structural and electronic properties, dynamics, and molecular interactions is required. The most popular model systems for self-assembly are alkanethiols on Au(111) substrates.[5] Unfunctionalized alkanethiols are the molecules most commonly used as an insulator or as a host for inserted conjugated molecules. However, the stability of alkanethiols on Au(111) is one of the most important issues for their applications in ambient environments where long-term use is required.[6]

The gold—thiolate bond degrades when exposed to air, UV light, or elevated temperatures.[7−11] In 1992, Tarlov and Newman discovered, using static secondary ion mass spectrometry, that alkanethiolates SAMs exposed to ambient environment experience oxidation of the sulfur headgroup.[12] In contrast, such sulfonate species were not found in SAMs after long-term storage in UHV (ultrahigh vacuum) in the absence of light.[13,14] Further spectroscopy studies found that alkanethiolate SAMs on gold can be easily oxidized to alkanesulfinates and alkanesulfides after exposure to ambient conditions.[9,12,15,16] These compounds are not chemisorbed but instead weakly

bonded to the surface leading to a deterioration of the alkanethiolate SAM.[11] Other studies suggest scissoring of the S—C bond due to oxidation leading to desorption of alkyl chain fragments and oxidation of the surface-bound sulfur.[17,18]

After these findings it was concluded that light and the presence of oxygen could remove alkanethiolate SAMs from the gold surface. Further exploration revealed that ozone is the main oxidant for thiolate SAM degradation.[10,19−21] Schoenfisch and Pemberton exposed alkanethiol SAMs to different gases and liquids, N_2, pure O_2, enclosed pressurized air, and O_3.[10] Only the SAMs exposed to ozone were oxidized. Other studies showed that oxidation of the surface occurs in the absence of light, provided that the sample is exposed to air.[9,11,22] The rate of oxidation depends on the morphology of the surface, the concentration of oxidants (e.g., ozone) in the ambient atmosphere, and the alkyl chain length.[22−25] When oxidized the SAMs lose their ordered, oriented upright nature and form laying-down or disordered phases.[21,26]

The decanethiol SAM on Au(111) has served as a prototypical model system for self-assembly and is therefore extensively studied.[27−31] By using scanning tunneling microscopy (STM), six different phases were found in the decanethiol SAM depending on the coverage.[32−34] In five of the six phases the decanethiolate molecules are lying down flat on the surface.

These five phases are a disordered lattice gas phase (α), a liquid phase (ϵ), and three striped phases: the centered $(23 \times \sqrt{3})$ phase (β), the centered $(19 \times \sqrt{3})$ phase (χ), and the hexagonal $(5\sqrt{3} \times \sqrt{3})R30°$ phase (δ). The sixth phase is the centered $(3 \times 2\sqrt{3})$ standing up phase (ϕ), which is found at full coverage. In real-space images of decanethiol self-assembled monolayers one often finds a coexistence of several phases, mixed phases, antiphase boundaries, vacancy islands, and ad-islands.[35−37] In previous studies we have investigated the stability of these SAMs revealing dynamic behavior within the monolayer showing that also SAMs are dynamic at room temperature.[30,31]

Although many studies probed the oxidation process of thiolate-based molecules, only a few studies reveal, using real-space techniques, what exactly happens on the surface when oxidation of the molecules occurs.[21,26] Recently, Ito et al.[26] showed that not only oxygen but also hydrogen can be the cause of instabilities and degradation of thiolate-based SAMs. In this work, we perform STM measurements on decanethiolate SAMs to further explore the oxidation process of thiolate-based molecules and the influence of the oxidation on the molecular order. We show that the decanethiolates first align in a stripelike fashion. When exposed to air, degradation of the gold−thiolate bond occurs transforming the decanethiolates into decanesulfonates which lie physisorbed on the Au(111) surface forming a lamellae-like structure. Both decanethiolates and decanesulfonates coexist on the surface and do not intermix.

METHODS

Experimental Details. An overview of the methods is given below; details are provided in the Supporting Information. Decanethiol (purity ≥99%) was purchased from Sigma-Aldrich (Steinheim, Germany) and used without further purification. The platform used for STM and XPS measurements was 11×11 mm^2, 250 nm Au on 2 nm Cr on borosilicate glass, purchased from Arrandee (Werther, Germany). Au(111) samples were obtained by annealing these substrates in a high-purity H$_2$ flame for 5 min. Decanethiol SAMs were obtained at room temperature by chemisorption from a 1 mM ethanolic solution onto freshly prepared Au(111) substrates for 24 h. This immersion step leads to a densely packed SAM where the decanethiolate molecules form a standing up phase. In order to reduce the coverage, we immersed our sample in a pure ethanol solution for 1 h. After thorough rinsing of the decanethiol SAMs with pure spectroscopy grade ethanol, the samples were loaded into UHV STM for imaging (RHK Technology UHV3000 variable temperature STM operating at a base pressure of 1×10^{-10} mbar, using chemical etched W tips). All measurements are acquired at room temperature. To check the presence of the SAMs on the Au(111) surface, contact angle measurements were carried out. The measured contact angle was $89 \pm 2°$ (see the Supporting Information for contact angle details for every stage in the preparation process). This result is in agreement with the observations of Li et al.[38] STM topography for the freshly annealed Au surface showed the herringbone reconstruction characteristic of clean Au(111). The oxidized samples were obtained by storing a freshly prepared reduced coverage sample under ambient laboratory conditions in air for up to 2 weeks (20 °C and $37 \pm 1\%$ humidity, measured with a ENSIRION EK-H4 SHTXX, Humidity Sensors, Eval Kit, SENSIRION, Switzerland). A

wooden container prevented the exposure of light to the sample but allowed air in. After 2 weeks of storage, the sample was placed in UHV STM for imaging.

Computational Details. SAM structures were calculated using the VASP program[39] with the GGA-PBE functional,[40] projector augmented wave (PAW) pseudopotentials[41] with a plane wave cutoff of 400 eV, and a vacuum spacing of at least 3 nm in the direction normal to the gold surface. The $26 \times \sqrt{3}$ a unit cell seen in the STM images is used as the simulation cell and contains four molecules adsorbed on a three-layer model of Au(111), 284 atoms, with the bottom layer of gold frozen to approximate the underlying bulk. The orthorhombic cells are of dimension $7.5 \times 0.5 \times 5.0$ nm and are replicated in all dimensions using periodic boundary conditions. Molecule−surface binding energies were converged to below 100 meV using a 12 k-point grid. The contributions of van der Waals physisorption to the overall molecule−surface binding energies were estimated using dDsC dispersion corrections.[42]

RESULTS AND DISCUSSION

Prior to the oxidation experiment, first the decanethiol SAM on Au(111) is investigated. Figure 1A shows Au(111) substrate
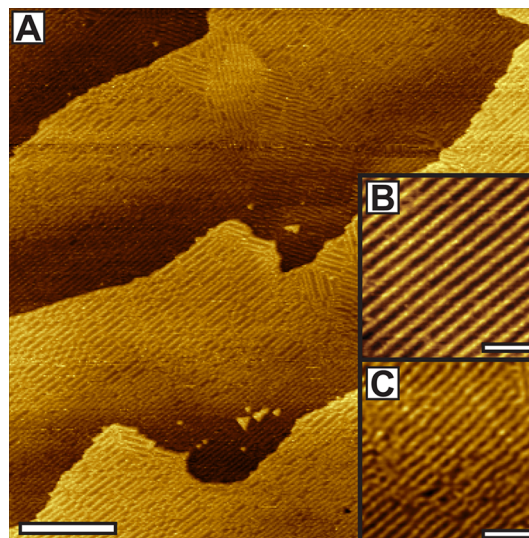

Figure 1. (A) STM topography image (210×210 nm^2) of decanethiol SAM on Au(111) showing the various phases at room temperature. Most of the terraces are covered with the β or δ phase. The tunneling parameters are 190 pA and 1.20 V, scale bar is 40 nm. (B) Zoomed image (35×35 nm^2) of the β phase. The separation between the stripes is 3.3 nm (scale bar is 10 nm). (C) Zoomed image (35×35 nm^2) of the δ phase with a stripe separation of 2.2 nm (scale bar is 10 nm).

with various decanethiol phases present on the surface in coexistence with several characteristic defects, such as substrate steps, ad-islands, and vacancy islands. The ad-islands (vacancy islands) are exactly one atomic layer high (2.5 Å), revealing that both features are defects within the Au(111) surface and not in the decanethiol SAM. On the terraces mainly two phases are observed, the β and δ phases, which coexist on the surface in agreement with previous studies.[29,32] The β phase (see Figure 1B) is a centered $(23 \times \sqrt{3})$ striped phase where the decanethiols lie down flat on the surface in an alternating head-to-head and tail-to-tail registry. The β phase has an interstripe distance of 3.3 nm, equal to two times the

decanethiol length, and a 0.49 nm periodicity along the stripes, equal to $\sqrt{3}$ times the Au(111) lattice constant a (2.884 Å). The β phase can shift perpendicular to the row direction by roughly half of the row spacing.

The δ phase (see Figure 1C) has an out-of-plane interdigitation configuration very comparable to the β phase; however, the tails are tilted approximately 30° from the surface normal. This leads to a smaller interstripe distance of 2.2 nm, and the unit cell is hexagonal $(5\sqrt{3} \times \sqrt{3})$R30°.[29] Similar to the β phase, the sulfur atoms are separated by the nearest-neighbor distance $\sqrt{3}\,a$, i.e., 0.49 nm. In a previous study we have revealed the dynamic behavior of the decanethiols at room temperature within these well-ordered phases using current–time $(I(t))$ spectroscopy.[30,31,43,44] The phases can undergo significant changes, shifting and transitioning between the various phases including a disordered phase.

X-ray photoelectron spectroscopy (XPS) was used to determine the change of the surface-chemical composition following exposure of the decanethiol monolayer to ambient conditions. A series of XPS spectra of the O 1s, S 2p, and the C 1s regions is shown in Figure 2. Photoemission spectra of the O
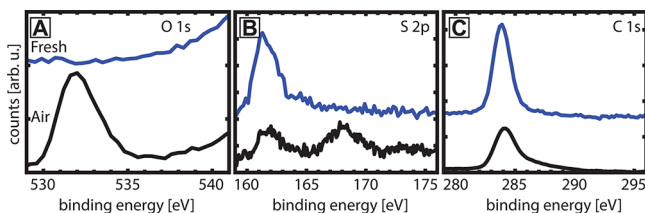

Figure 2. XPS spectra obtained from decanethiol SAMs on Au(111). Spectra in blue are from a fresh sample while spectra in black are from a sample exposed for 2 weeks to ambient conditions. (A) Spectra of the O 1s region showing that the monolayer exposed to air contains oxygen in contrast to the fresh sample. (B) Spectra of the S 2p region showing a reduced intensity of the S–Au bond peak in the air-exposed sample. A second peak appears corresponding to oxidized S species. (C) Spectra of the C 1s region showing that the monolayer exposed to air exhibits loss of carbon intensity.

1s binding energy region (Figure 2A) indicate that thiolate molecules that are not exposed to air exhibit no detectable oxygen. Following oxidation a peak arises at 532 eV, characteristic of O 1s,[18,23] indicating the incorporation of oxygen into the material.

The fresh sample contains primarily a spin–orbit split doublet with S $2p_{3/2}$ at 162 eV binding energy in the XPS spectra (Figure 2B) which is characteristic of thiolates on Au.[10,11,45,46] When exposed to air, the 162 eV peak decreases in intensity, and a new feature at 168 eV emerges. The 168 eV peak is assigned to oxidized sulfur species.[10,18] This suggests that both decanethiols as well as oxidized species are simultaneously present on the surface. Photoemission spectra acquired from the C 1s binding energy region (Figure 2C) indicate that the monolayer exposed to air exhibits a decrease of the C 1s intensity. Loss of intensity is attributed to a fraction of the molecules that desorb during oxidation in line with the reports of Poirier et al. and Schoenfisch and Pemberton.[10,21]

In Figure 3A a scanning tunneling microscopy image is shown of a self-assembled decanethiol monolayer on Au(111) after 2 weeks of exposure to ambient conditions. In contrast to the surface prior to oxidation, the terraces are no longer completely covered with decanethiol phases. The β phase is still
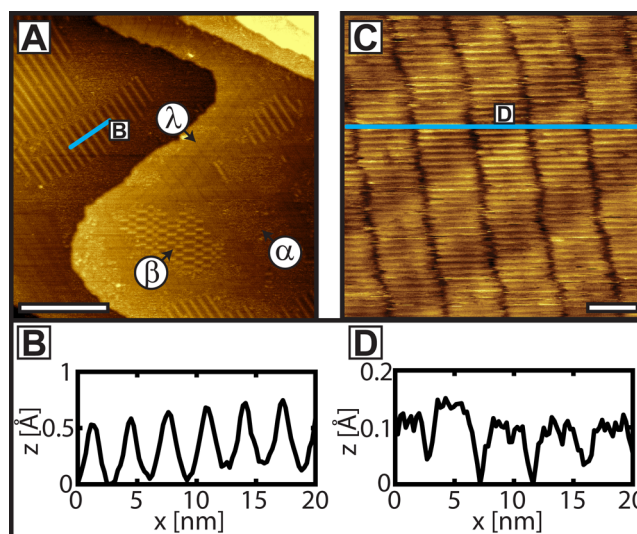

Figure 3. (A) STM topography image $(100 \times 100 \text{ nm}^2)$ of decanethiol SAM on Au(111) after 2 weeks of exposure to ambient conditions. Both the β and a fluid phase (α) are present on the surface. The different domains of decanethiol phases are separated by the oxidized decanethiol phase (λ phase). The λ phase is composed of fine-striped domains with a width of about 3.5 nm separated by vacancy lines which run perpendicular to the fine stripes. The tunneling parameters are 190 pA and 1.20 V, scale bar is 30 nm. (B) Cross-sectional height profile from corresponding line segment in (A) shows 3.3 nm corrugation periodicity of the β phase. (C) Zoomed image $(20 \times 20 \text{ nm}^2)$ of the λ phase. The herringbone reconstruction of the Au(111) surface is preserved indicating a weak interaction between the molecules and the surface. Tunneling current 55 pA, sample bias 200 mV, scale bar 3 nm. (D) Cross-sectional height profile from corresponding line segment in (B) revealing a 3.5 nm width of the fine-striped domains.

present on the surface, whereas the δ phase has disappeared. Instead a significant fraction of the near-surface region converted into a fluidlike phase. The fluidlike phase has no periodic order, and the molecules diffuse around the surface.[21,30] This is in good agreement with the observed changes in the XPS data. A decrease in the intensity of the C 1s peak is observed which is attributed to the desorption of molecules during oxidation (Figure 2C). Desorption leads to a lower surface coverage and thus to phases with a lower density (for example the β phase). Therefore, the high-density δ phase disappears after oxidation, and the low-density fluid phase arises. The cross-sectional height profile in Figure 3B shows that the interstripe spacing in the β phase remains approximately 33 Å. In addition to the two decanethiol phases, another stripelike phase is present on the surface. For now we will refer to this phase as the λ phase.

Figure 3C shows a zoomed image of the λ phase. The herringbone structure of the underlying Au(111) substrate is visible underneath the ordered molecular layer. The herringbone reconstruction contains 46 atoms in the top layer placed on 44 atoms of the second layer resulting in a $(22 \times \sqrt{3})$ unit cell.[47] The unit cell consists of alternating fcc and hcp domains that exhibit a slightly elevated ridge with a height of about 15 pm. Both the herringbone periodicity and the fcc/hcp ratio are unaltered compared to the bare gold surface. The herringbone reconstruction is a sensitive readout of the molecule–surface interaction strength.[48,49] When the molecules interact with the Au(111) surface, the herringbone periodicity becomes larger

until it eventually completely vanishes. Therefore, there must be a rather weak interaction between the molecules and the Au(111) substrate.

The λ phase is composed of fine-striped domains with a width of approximately 3.5 nm separated by vacancy lines which run perpendicular to the fine stripes (see Figure 3D). The stripes are aligned along one of the closed packed directions of the Au(111) substrate ($\langle 01\bar{1}\rangle$). The fine-stripe direction makes an angle of 30° with the ridges of the herringbone reconstruction (which run in $\langle 11\bar{2}\rangle$ directions). The separation between the fine stripes is $\sqrt{3}\,a$, i.e., 0.5 nm. The fine stripes of neighboring domains are always out-of-phase. The XPS spectra of the S 2p core region shows two peaks for the oxidized sample. The decanethiol phases are still present on the surface explaining the peak at 162 eV. The second peak at 168 eV is assigned to oxidized sulfur species. Since the λ phase is only observed after exposure to air, we assume that the molecules in the λ phase are oxidized. In addition, previous studies on decanethiol SAMs characterized all of the structural phases for decanethiols on Au(111) including phases due to annealing or oxidation.[21,29,32] None of the observed phases matches the characteristics of the λ phase. Poirier et al. investigated the oxidation process using STM.[21] However, they were unable to find a structured phase of oxidized decanethiols. The oxidation procedure was different compared to the procedure followed in this study. Instead of using air, they performed their experiments in an ozone environment. This probably results into a lower density of oxidized molecules on the surface and thus to a disordered rather than an ordered phase.

The exact mechanism of oxidation is still under debate. Lewis et al.[17] proposed S−C scissoring followed by desorption of the alkyl fragment leaving oxidized sulfur on the Au(111) surface. However, we find zero evidence for ordered domains of oxidized sulfur in our STM data. The second oxidation process proposed is the formation of alkanesulfinates and alkanesulfides.[9,12,15,16] These species are less strongly bound to the surface due to the reduced nucleophilicity of the sulfur anchoring group. In our case most probably the end of the decanethiol is transformed from a thiolate into a sulfonate given the S 2p$_{3/2}$ peak position after oxidation (Figure 2B). The peak is positioned around 168 eV which corresponds to sulfonates (sulfinates features are seen around 166.5 eV[22]). The change of the end group of the molecule also triggers a reorientation of the molecules with respect to the surface normal. The tilt angles fall away from the surface normal leading to molecules laying flat on the surface like in the λ phase.

The λ phase looks very similar to the previous observed alkane and alkanol monolayers on Au(111).[50−52] These molecules adopt a similar lamellar structure where the alkanes/alkanols molecules are packed side-by-side to form commensurate structures with respect to the reconstructed Au(111) surface. The herringbone is unaffected and is visible through the monolayer. In these structures every rod is composed of one alkane/alkanol molecule with a thickness of approximately 0.5 nm. The rod thickness in the λ phase is also 0.5 nm ($\sqrt{3}\,a$) while the width is 3.5 nm, approximately twice the length of a decanethiol (1.695 nm[53]). The height variation in the λ phase (see Figure 3D) is similar to the alkanol monolayer but much smaller compared to the β phase (see Figure 3B). In the β phase the sulfur atoms appear brighter than the alkyl chains due to mixing of the orbitals of the sulfur

atom and the gold surface.[54] Therefore, we propose that in the λ phase, the rods consist of two decanesulfonates, where the sulfur atoms are bonded to three oxygen atoms (see Figure 4A
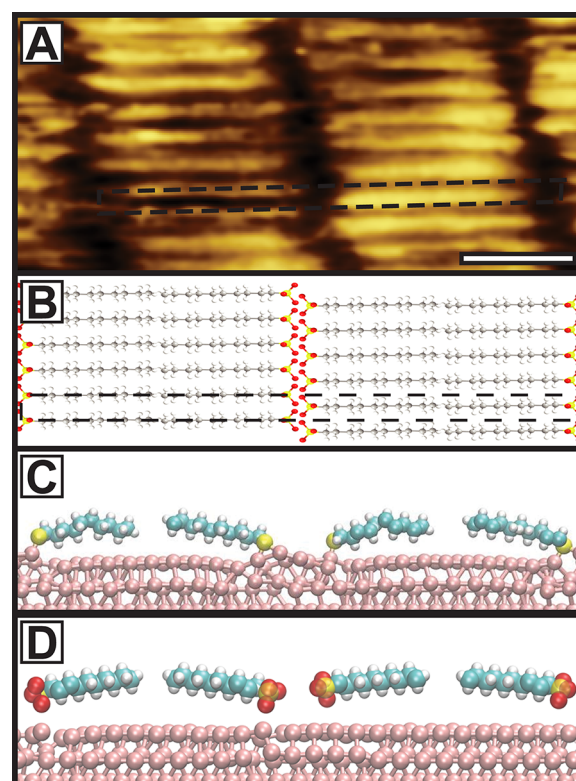

Figure 4. (A) Zoomed topography image (10 × 10 nm²) of the decanesulfonate phase. Tunneling current 55 pA, sample bias 200 mV, scale bar 2 nm. (B) Proposed structure of the λ phase. The rods consist of two decanesulfonates. The unit cell is $26 \times \sqrt{3}\,a$ (dashed black box) and contains two rods with a thickness of $\sqrt{3}\,a$ which are out of phase. The white and gray circles refer to hydrogen and carbon atoms, respectively, while red is oxygen and yellow refers to a sulfur atom. (C) DFT calculations of chemisorbed decanethiol molecules and (D) of the physisorbed decanesulfonates structure. When the sulfur becomes oxidized, the molecule−surface interaction energy drops from −3.4 to −0.4 eV, respectively.

and B). Because the sulfur atom is bonded to three oxygen atoms, no mixing of orbitals occurs, and no height difference is observed. Also no gap is observed between the two adjacent molecules which is most probably caused by the asymmetrical form of the CH$_3$ groups. The inequivalent position of the CH$_3$ tail groups relative to the molecule axis (i.e., one CH$_3$ group is higher than the other) results in the same current contrast on the alkyl chain and in between them.[55] On the sulfonate side of the molecules, a vacancy line is created.

The herringbone reconstruction is still present on the surface excluding any strong interaction between the sulfonate group and the Au(111) lattice. This is confirmed by density functional theory (DFT) calculations, which show the formation of chemisorbed $26 \times \sqrt{3}\,a$ SAM structures for decanethiolate molecules (Figure 4C and Figure S8 in the Supporting Information for the case of the adatom model) that weaken to physisorbed structures (Figure 4D) as the sulfur becomes oxidized, in agreement with both STM and XPS data. The computed molecule−surface interaction energy drops from −3.4 eV (−2.2 eV chemisorption with 2.4 Å Au−S covalent

bonds plus −1.2 eV physisorption; Figure 4C) to −0.4 eV (purely physisorbed with zero chemisorption; Figure 4D). The lower molecule−surface interaction (and especially the absence of any chemisorption between the molecules and the surface) explains the observed herringbone reconstruction underneath the decanesulfonate SAM. The strong covalent Au−S bond leads to charge accumulation and consequently to a depletion of charge that is available for the bonding of the Au atom with its neighboring Au atoms.[56] This results in a dramatic decrease of the strong tensile stress among the Au atoms, leading to the deconstruction of the Au(111) surface. When the sulfur atom of the decanethiol is oxidized, no covalent bond is formed and therefore the herringbone reconstruction is unaltered. The decanesulfonates are arranged in a $26 \times \sqrt{3}\,a$ unit cell, which contains two rods (four molecules). When scanning tunneling spectroscopy is performed on every position on top of these rods, a semiconducting current−voltage, i.e., $I(V)$, signature is measured (see the Supporting Information).

Although ease of preparation and stability of alkanethiols SAMs on gold are thus far unmatched by any other system for SAM formation, the often made assumption that the gold−sulfur bond is ultrarobust and stable under ambient conditions is false. The instability of the decanethiol monolayer at room temperature and the process of oxidation at ambient conditions have a huge impact on the structure of the monolayer, which is highly undesirable for ambient condition electronics. However, the oxidized decanethiol (decanesulfonates) molecules form a new phase which shows no structural fluctuations within the monolayer.

CONCLUSIONS

In summary, we have studied the oxidation process of self-assembled alkanethiol monolayers on gold using STM and XPS. Often it is assumed that the gold−sulfur bond is robust and stable under ambient conditions, but we show that this is not the case. The decanethiol SAMs have the tendency to oxidize when the monolayer is in contact with air. The fresh decanethiol monolayer consists mainly out of two phases, the low-density β phase and the high-density δ phase. Air-exposed SAMs oxidize, as seen in the chemical shift of the S 2p and the appearance of O 1s photoelectrons. When the monolayer is exposed to ambient conditions, part of the decanethiol monolayer transforms into decanesulfonates. The decanesulfonates lie flat on the surface in a lammelae-like structure (λ phase) and have a weak interaction with the substrate. The herringbone reconstruction of the Au(111) remains intact, and the SAM structures are remarkably stable at ambient conditions. These results show the influence of oxidation on the alkanethiol monolayer.

ASSOCIATED CONTENT

Ⓢ Supporting Information

The Supporting Information is available free of charge on the ACS Publications website at DOI: 10.1021/acs.jpcc.8b01389.

> Contact angles through the preparation process; $I(V)$ spectroscopy on the λ phase; XPS: the complete XPS spectra of the fresh and air exposed sample; computed SAM structures: full details of the density functional theory (DFT) calculations (PDF)

AUTHOR INFORMATION

Corresponding Author
*E-mail: k.sotthewes@utwente.nl, sotthewes@physik.rwth-aachen.de, phone: +31534893961

ORCID Ⓞ
Kai Sotthewes: 0000-0003-2073-6958
Jurriaan Huskens: 0000-0002-4596-9179

Present Address
⊥Institute of Enhanced Oil Recovery, China University of Petroleum (Beijing), Beijing 102249, P. R. China

Notes
The authors declare no competing financial interest.

ACKNOWLEDGMENTS

REFERENCES

(1) De Feyter, S.; De Schryver, C. Two-dimensional supramolecular self-assembly probed by scanning tunneling microscopy. *Chem. Soc. Rev.* **2003**, *32*, 139−150.

(2) McCreery, R. L. Molecular electronic junctions. *Chem. Mater.* **2004**, *16*, 4477.

(3) Love, J.; Estroff, L.; Kriebel, J.; Nuzzo, R.; Whitesides, G. Self-assembled monolayers of thiolates on metals as a form of nanotechnology. *Chem. Rev.* **2005**, *105*, 1103.

(4) Sotthewes, K.; Geskin, V.; Heimbuch, R.; Kumar, A.; Zandvliet, H. J. W. Research update: Molecular electronics: The single-molecule switch and transistor. *APL Mater.* **2014**, *2*, 010701.

(5) Vericat, C.; Vela, M.; Benitez, G.; Carro, P.; Salvarezza, R. Self-assembled monolayers of thiols and dithiols on gold: New challenges for a well-known system. *Chem. Soc. Rev.* **2010**, *39*, 1805.

(6) Srisombat, L.; Jamison, A.; Lee, T. R. Stability: A key issue for self-assembled monolayers on gold as thin-film coatings and nanoparticle protectants. *Colloids Surf., A* **2011**, *390*, 1−19.

(7) Garrell, R. L.; Chadwick, J. E.; Severance, D. L.; McDonald, N. A.; Myles, D. C. Adsorption of sulfur containing molecules on gold: The effect of oxidation on monolayer formation and stability characterized experiments and theory. *J. Am. Chem. Soc.* **1995**, *117*, 11563−11571.

(8) Horn, A. B.; Russel, D. A.; Shorthouse, L. J.; Simpson, T. R. E. Ageing of alkanethiol self-assembled monolayer. *J. Chem. Soc., Faraday Trans.* **1996**, *92*, 4759−4762.

(9) Scott, J. R.; Baker, L. S.; Everett, W. R.; Wilkins, C. L.; Fritsch, I. Laser desorption fourier transform mass spectrometry exchange studies of air-oxidized alkanethiol self-assembled monolayers on gold. *Anal. Chem.* **1997**, *69*, 2636−2639.

(10) Schoenfisch, M. H.; Pemberton, J. E. Air stability of alkanethiol self-assembled monolayers on Silver and Gold Surfaces. *J. Am. Chem. Soc.* **1998**, *120*, 4502−4513.

(11) Willey, T. M.; Vance, A. L.; van Buuren, T.; Bostedt, C.; Terminello, L. J.; Fadley, C. S. Rapid degradation of alkanethiol-based self-assembled monolayers on gold in ambient laboratory conditions. *Surf. Sci.* **2005**, *576*, 188−196.

(12) Tarlov, M. J.; Newman, J. G. Static secondary ion mass spectrometry of self-assembled alkanethiol monolayers on gold. *Langmuir* **1992**, *8*, 1398−1405.

(13) Rieley, H.; Price, N. J.; Smith, T. L.; Yang, S. Photo-oxidation and photo-reduction in alkylthiol monolayers self-assembled on gold. *J. Chem. Soc., Faraday Trans.* **1996**, *92*, 3629−3634.

(14) Noh, J.; Kato, H. S.; Kawai, M.; Hara, M. Surface structure and interface dynamics of alkanethiol self-assembled monolayers on Au(111). *J. Phys. Chem. B* **2006**, *110*, 2793−2797.

(15) Li, Y.; Huang, J.; McIver, R. T., Jr.; Hemminger, J. C. Characterization of thiol self-assembled films by laser desorption fourier transform mass spectrometry. *J. Am. Chem. Soc.* **1992**, *114*, 2428−2432.

(16) Burroughs, J. A.; Hanley, L. Laser desorption ion trap mass spectrometry of selfassembled monolayers. *J. Am. Soc. Mass Spectrom.* **1993**, *4*, 968−970.

(17) Lewis, M.; Tarlov, M.; Carron, K. Study of photooxidation process of self-assembled alkanethiol monolayers. *J. Am. Chem. Soc.* **1995**, *117*, 9574−9575.

(18) Hutt, D. A.; Cooper, E.; Leggett, G. J. Structure and mechanism of photooxidation of self-assembled monolayers on alkylthiols on silver studied by XPS and Static SIMS. *J. Phys. Chem. B* **1998**, *102*, 174−184.

(19) Norrod, K. L.; Rowlen, K. L. Ozone-induced oxidation of self-assembled decanethiol: Contributing mechanism for "photooxidation"? *J. Am. Chem. Soc.* **1998**, *120*, 2656−2657.

(20) Zhang, Y.; Terrill, R. H.; Tanzer, T. A.; Bohn, P. W. Ozonolysis is the primary cause of UV photooxidation of alkanethiolate monolayers at low irradiance. *J. Am. Chem. Soc.* **1998**, *120*, 2654−2655.

(21) Poirier, G. E.; Herne, T. M.; Miller, C. C.; Tarlov, M. J. Molecular-scale characterization of the reaction of ozone with decanethiol monolayers on Au(111). *J. Am. Chem. Soc.* **1999**, *121*, 9703−9711.

(22) Lee, M.-T.; Hsueh, C.-C.; Freund, M. S.; Ferguson, G. S. Air oxidation of self-assembled monolayers on polycrystalline gold: The role of the gold substrate. *Langmuir* **1998**, *14*, 6419−6423.

(23) Hutt, D. A.; Leggett, G. J. Influence of adsorbate ordering on rates of UV photooxidation of self-assembled monolayers. *J. Phys. Chem.* **1996**, *100*, 6657−6662.

(24) Wang, M. C.; Liao, J. D.; Weng, C. C.; Klauser, R.; Shaporenko, A.; Grunze, M.; Zharnikov, M. Modification of aliphatic monomolecular films by free radical dominant plasma: the effect of the alkyl chain length and the substrate. *Langmuir* **2003**, *19*, 9774−9780.

(25) Cortes, E.; Rubert, A. A.; Benitez, G.; Carro, P.; Vela, M. E.; Salvarezza, R. C. Enhanced stability of thiolate self-assembled monolayers (SAMs) on nanostructured gold substrates. *Langmuir* **2009**, *25*, 5661−5666.

(26) Ito, E.; Kang, H.; Lee, D.; Park, J. B.; Hara, M.; Noh, J. Spontaneous desorption and phase transitions of self-assembled alkanethiol and alicyclic thiol monolayers chemisorbed on Au(111) in ultrahigh vacuum at room temperature. *J. Colloid Interface Sci.* **2013**, *394*, 522−529.

(27) Schreiber, F.; Eberhardt, A.; Leung, T.; Schwartz, P.; Wetterer, S.; Lavrich, D.; Berman, L.; Fenter, P.; Eisenberger, P.; Scoles, G. Adsorption mechanisms, structures, and growth regimes of an archetypal self-assembled system: Decanethiol on Au(111). *Phys. Rev. B: Condens. Matter Mater. Phys.* **1998**, *57*, 12476.

(28) Staub, R.; Toerker, M.; Fritz, T.; Schmitz-Hubsch, T.; Sellam, F.; Leo, K. Flat lying pin-stripe phase of decanethiol self-assembled monolayers on Au(111). *Langmuir* **1998**, *14*, 6693.

(29) Qian, Y.; Yang, G.; Yu, J.; Jung, T.; Liu, G. Structures of annealed decanethiol self-assembled monolayers on Au(111): an ultrahigh vacuum scanning tunneling microscopy study. *Langmuir* **2003**, *19*, 6056.

(30) Wu, H. R.; Sotthewes, K.; Kumar, A.; Vancso, G. J.; Schön, P. M.; Zandvliet, H. J. W. Dynamics of decanethiol self-assembled monolayers on Au(111) studied by time-resolved scanning tunneling microscopy. *Langmuir* **2013**, *29*, 2250.

(31) Sotthewes, K.; Wu, H. R.; Kumar, A.; Vancso, G. J.; Schön, P. M.; Zandvliet, H. J. W. Molecular dynamics and energy landscape of

decanethiolates in self-assembled monolayers on Au(111) studied by scanning tunneling microscopy. *Langmuir* **2013**, *29*, 3662.

(32) Poirier, G. E. Coverage-dependent phases and phase stability of decanethiol on Au(111). *Langmuir* **1999**, *15*, 1167−1175.

(33) Poirier, G. E.; Fitts, W. P.; White, J. M. Two-dimensional phase diagram of decanethiol on Au(111). *Langmuir* **2001**, *17*, 1176.

(34) Fitts, W.; White, J.; Poirier, G. Low-coverage decanethiolate structure on Au(111): Substrate effects. *Langmuir* **2002**, *18*, 1561.

(35) Toerker, M.; Staub, R.; Fritz, T.; Schmitz-Hubsch, T.; Sellam, F.; Leo, K. Annualed decanethiol monolayers on Au(111): Intermediate phases between structures with high and low molecular surface denisty. *Surf. Sci.* **2000**, *445*, 100.

(36) Schreiber, F. Structure and growth of self-assembling monolayers. *Prog. Surf. Sci.* **2000**, *65*, 151.

(37) Yamada, R.; Uosaki, K. In situ scanning tunneling microscopy observation of the self-assembly process of alkanethiols on Gold(111) in Solution. *Langmuir* **1998**, *14*, 855.

(38) Li, S.-S.; Xu, L.-P.; Wan, L.-J.; Wang, S.-T.; Jiang, L. Time-dependent organization and wettability of decanethiol self-assembled monolayer on Au(111) investigated with STM. *J. Phys. Chem. B* **2006**, *110*, 1794−1799.

(39) Kresse, G.; Hafner, J. Ab initio molecular dynamics for liquid metals. *Phys. Rev. B: Condens. Matter Mater. Phys.* **1993**, *47*, 558−561.

(40) Perdew, J. P.; Burke, K.; Ernzerhof, M. Generalized gradient approximation made simple. *Phys. Rev. Lett.* **1996**, *77*, 3865−3868.

(41) Blöchl, P. E. Projector augmented-wave method. *Phys. Rev. B: Condens. Matter Mater. Phys.* **1994**, *50*, 17953−17979.

(42) Steinmann, S. N.; Corminboeuf, C. Comprehensive benchmarking of a density-dependent dispersion correction. *J. Chem. Theory Comput.* **2011**, *7*, 3567−3577.

(43) Sotthewes, K.; Heimbuch, R.; Zandvliet, J. W. H. Manipulating transport through a single-molecule junction. *J. Chem. Phys.* **2013**, *139*, 214709.

(44) Sotthewes, K.; Heimbuch, R.; Zandvliet, H. J. W. Dynamics of copper-phthalocyanine molecules on Au/Ge(001). *J. Chem. Phys.* **2015**, *143*, 134303.

(45) Laibinis, P. E.; Whitesides, G. M.; Allara, D. L.; Tao, Y.-T.; Parikh, A. N.; Nuzzo, R. G. Comparison of the structures and wetting properties of self-assembled monolayers of n- alkanethiols on the coinage metal surfaces, Cu, Ag. *J. Am. Chem. Soc.* **1991**, *113*, 7152−7167.

(46) Zharnikov, M. High-resolution X-ray photoelectron spectroscopy in studies of self-assembled organic monolayers. *J. Electron Spectrosc. Relat. Phenom.* **2010**, *178−179*, 380−393.

(47) Wöll, C.; Chiang, S.; Wilson, R. J.; Lippel, P. H. Determination of atom positions at stacking-fault dislocations on Au(111) by scanning tunneling microscopy. *Phys. Rev. B: Condens. Matter Mater. Phys.* **1989**, *39*, 7988−7991.

(48) Rossel, F.; Brodard, P.; Patthey, F.; Richardson, N. V.; Schneider, W.-D. Modified herringbone reconstruction on Au(111) induced by self-assembled Azure A island. *Surf. Sci.* **2008**, *602*, L115−L117.

(49) Jewell, A. D.; Kyran, S. J.; Rabinovich, D.; Sykes, E. C. H. Effect of head-group chemistry on surface-mediated molecular self-assembly. *Chem. - Eur. J.* **2012**, *18*, 7169−7178.

(50) Zhang, H.-M.; Yan, J.-W.; Xie, Z.-X.; Mao, B.-W.; Xu, X. Self-Assembly of alkanols on Au(111) surfaces. *Chem.- Eur. J.* **2006**, *12*, 4006−4013.

(51) Zhang, H.-M.; Xie, Z.-X.; Mao, B.-W.; Xu, X. Self-assembly of normal alkanes on the Au (111) surface. *Chem. - Eur. J.* **2004**, *10*, 1415−1422.

(52) Xie, Z.-X.; Huang, Z.-F.; Xu, X. Influence of reconstruction on the structure of self-assembled normal-alkane monolayers on Au(111) surfaces. *Phys. Chem. Chem. Phys.* **2002**, *4*, 1486−1489.

(53) Camillone, N., III; Leung, T. Y. B.; Schwartz, P.; Eisenberger, P.; Scoles, G. Chain length dependence of the striped phases of alkanethiol monolayers self-assembled on Au(111): An atomic beam diffraction study. *Langmuir* **1996**, *12*, 2737−2746.

(54) Zeng, C.; Li, B.; Wang, B.; Wang, H.; Wang, K.; Yang, J.; Hou, J. G.; Zhu, Q. What can a scanning tunneling microscope image do for the insulating alkanethiol molecules on Au(111) substrates? *J. Chem. Phys.* **2002**, *117*, 851.

(55) Marchenko, A.; Lukyanets, S.; Cousty, J. Adsorption of alkanes on Au(111): Possible origin of STM contrast at the liquid/solid interface. *Phys. Rev. B: Condens. Matter Mater. Phys.* **2002**, *65*, 045414.

(56) Shih, Y.-C.; Chen, C.-S.; Wu, K.-C. First-principles surface stress calculations and multiscale deformation analysis of a self-assembled monolayer adsorbed on a micro-cantilever. *Sensors* **2014**, *14*, 7435−7450.